Prandtl number effects on mixing in Kelvin-Helmholtz billows

Mona Rahmani, Brian Seymour, Gregory Lawrence

University of British Columbia
mrahmani@math.ubc.ca

Abstract

We use DNS to study the effect of Prandtl number on mixing in weakly density stratified Kelvin-Helmholtz (KH) billows at low to moderate Reynolds numbers. The time evolution of the density field of the flow and the mixing are significantly influenced by the Prandtl number. By increasing the Prandtl number, the final amount of mixing increases for Reynolds that are too low to sustain three-dimensional motions. Contrarily, the final amount of mixing decreases with increasing Prandtl number for sufficiently high Reynolds number KH flows that can develop significant three-dimensional motions. Our results indicate a steady increase in the total amount of mixing for buoyancy Reynolds numbers above 7, consistent with the results of Shih et al. (2005). Our measure of mixing efficiency exhibits a decreasing trend with increasing Prandtl number, in agreement with previous studies.

1 Introduction

An important source of mixing in stratified environmental flows is the turbulent breakdown of Kelvin-Helmholtz (KH) instabilities. A key parameter in determining the amount of mixing is the Prandtl number (Pr), the ratio of viscosity to molecular diffusivity of scalars. For different environments, Pr can vary over three decades, e.g. from 0.7 for heat in the atmosphere up to 700 for salt in the ocean. While the significance of Pr in characterizing mixing is widely acknowledged, the effect of Prandtl number on mixing is still not well understood. The reason is that high Prandtl number mixing phenomena require high-resolution numerical simulations or field and laboratory measurements which are still not achievable. Our goal here is to present some Prandtl number effects for low to moderate Reynolds number KH flows which are within reach of numerical simulations (see also Rahmani et al., 2016). Such flows are of interest in different environmental flows, for example the internal seiche induced KH instabilities in lakes (Rahmani et al., 2014b; Spigel and Imberger, 1980).

The primary KH billow is susceptible to the development of three-dimensional, secondary instabilities, which provide mechanisms for the transition to turbulence (Klaassen and Peltier, 1985; Mashayek and Peltier, 2012). The three-dimensional turbulent motions progressively contribute more to the generation of mixing over a range of Reynolds numbers referred to as the "mixing transition" (Konrad, 1977; Breidenthal, 1981; Koochesfahani and Dimotakis, 1986; Dimotakis, 2005; Rahmani et al., 2014a). Above the mixing transition three-dimensional motions are sustained and the dependence of mixing on Reynolds number is weak, while below the mixing transition three-dimensional instabilities are suppressed and mixing is Reynolds number dependent. Laboratory experiments performed at $Pr = 0.7$ (Konrad, 1977) and at $Pr = 700$ (Breidenthal, 1981; Koochesfahani and Dimotakis, 1986) exhibited the same range of transitional Reynolds numbers. At high Prandtl numbers the flow structures become finer resulting in an increase in the interfacial area and the potential for mixing (Schowalter et al., 1994; Atsavapranee and Gharib, 1997; Balmforth et al., 2012). However, the slower rate of molecular diffusivity

at higher Prandtl numbers might result in a reduced amount of mixing (Cortesi et al., 1999; Staquet, 2000; Smyth et al., 2001; Salehipour et al., 2015). In the present paper, we use DNS to examine these two competing effects as Prandtl number increases. We focus on higher Prandtl numbers: Pr = 1 - 64 in three-dimensions, and Pr = 1 - 700 in two dimensions. We examine the dependence of mixing and mixing efficiency on the Prandtl number and buoyancy Reynolds number, and compare our results to previous studies when data are available.

2 Governing equations and dimensionless parameters

The dimensionless Boussinesq Navier-Stokes and advection-diffusion equations are

$$\frac{D\boldsymbol{u}}{Dt} = -\nabla p - J\rho\hat{\mathbf{k}} + \frac{1}{Re_0}\nabla^2\boldsymbol{u}, \quad \text{and} \quad \nabla.\boldsymbol{u} = 0, \tag{1}$$

$$\frac{D\rho}{Dt} = \frac{1}{Re_0 Pr}\nabla^2\rho, \tag{2}$$

where $\boldsymbol{u}$ is the dimensionless velocity field, ρ is the dimensionless density field, p denotes the dimensionless pressure field, and $\hat{\mathbf{k}}$ is the unit vertical vector. We choose an initial flow with horizontal velocity and density profiles defined by

$$U(z) = \frac{1}{2}\tanh(2z), \qquad \text{and} \qquad \bar{\rho}(z) = -\frac{1}{2}\tanh(2Rz). \tag{3}$$

In the equations above the velocity field has been non-dimensionalized by ΔU, the horizontal velocity difference, the density field by $\Delta\rho$, the density difference across the interface, time by $\delta_0/\Delta U$, dimensions by δ_0, and pressure by $\rho_0\Delta U^2$, where δ_0 is the initial value for the time-varying vorticity interface thickness of δ, and ρ_0 is a reference density. $R = \delta_0/h_0$ is the scale ratio, with h_0 being the initial value for the time-varying density interface thickness of h. The dimensionless numbers for this flow are

$$Re_0 = \frac{\delta_0\Delta U}{\nu}, \quad J = \frac{\Delta\rho g\delta_0}{\rho_0\Delta U^2}, \quad \text{and} \quad Pr = \frac{\nu}{\kappa}, \tag{4}$$

the initial Reynolds number, the bulk Richardson number, and the Prandtl number, where g is the gravitational acceleration, ν is the kinematic viscosity, κ the molecular diffusivity. The scale ratio is related to the Prandtl number by $R = Pr^{1/2}$.

Detailed descriptions of the numerical simulations are given in Rahmani et al. (2016). So here we give a brief summary of the choices of dimensionless parameters. We chose Prandtl numbers of Pr = 1, 9, 16, 25, and 64 for three-dimensional simulations at Re_0 = 100, 300, 400, and 600. Simulation of Pr = 64 and Re_0 = 600 flow in three dimensions was not possible due to numerical resource limitations. We also performed simulations at Re_0 = 300, 400, and 600 in two dimensions. At Re_0 = 300, a two-dimensional simulation was also performed at Pr = 700. In all simulations the bulk Richardson number is J = 0.03. The height of the domain is L_z = 9 (non-dimensionalized by δ_0), and the width of the domain in three-dimensional simulations is $L_y = L_x/2$. Periodic horizontal and free-slip vertical boundary conditions are applied. The initial velocity and density profiles are perturbed using the eigenfunctions from the numerical solution of the linear stability equation. The initial velocity field is also perturbed with a small random noise that generates three-dimensional secondary instabilities. The grid spacing is smaller than $2.6L_B$, where L_B is the Batchelor length scale (Batchelor, 1959).

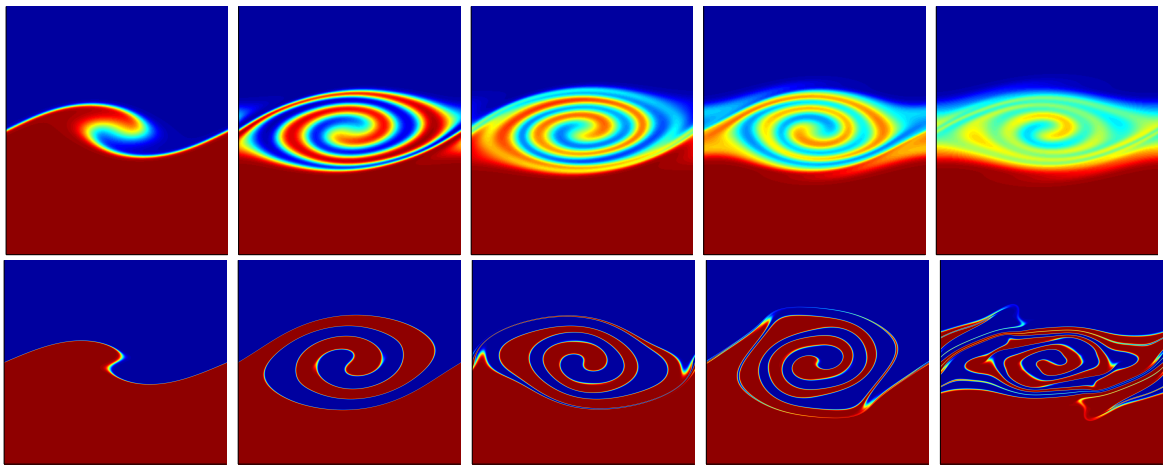

Figure 1: Snapshots of the density structure of the primary KH billow at $Re_0 = 300$ at different non-dimensional times $t = 20$, 50, 70, 80 and 100 from left to right and for $Pr = 9$ top row, and 700 bottom row.

3 Evolution of KH billow

Figure 1 shows how increasing the Prandtl number influences the evolution of the primary KH instability. Fine scale structures in the density field and sharp interfaces are seen in the $Pr = 700$ billow. These features are suppressed by diffusivity at $Pr = 9$. The differences in the evolution of these different Pr flows have significant implications for the type of three-dimensional instabilities that appear later in the flow and the transition to turbulence. More details on the effects of Prandtl number on the three-dimensional flow fields are given in Rahmani et al. (2016).

4 Mixing properties

It is well known that mixing properties depend on the buoyancy Reynolds number (Barry et al., 2001; Shih et al., 2005), the Prandtl number (Smyth et al., 2001; Nash and Moum, 2002; Salehipour et al., 2015) and the Richardson number (Fernando, 1991; Lozovatsky et al., 2006; Mashayek and Peltier, 2011), as well as the stage and nature of turbulence (Park et al., 1994; Balmforth et al., 1998). Shih et al. (Shih et al., 2005), identified different mixing regimes with increasing buoyancy Reynolds number: diffusive, intermediate and energetic. The mixing transition as described by Breidenthal (1981) and Koochesfahani and Dimotakis (1986) falls in the intermediate regime. In each regime, mixing efficiency had a distinct dependence on buoyancy Reynolds number and Prandtl number. Here, we examine the effects of the Prandtl number on mixing and mixing efficiency for diffusive and intermediate (or low and transitional) Reynolds numbers. Examining the Richardson number effects is however beyond the scope of the present work.

We quantify mixing, M, as the irreversible increase in the background potential energy, P_b, the minimum potential energy obtained when fluid particles are rearranged adiabatically to a stable state, $\rho(z^*)$, see Winters et al. (1995). We normalize P_b by the mean initial kinetic energy of the flow, i.e. $\rho_0 \Delta U^2$, and exclude diffusion of the initial background stratification at rate ϕ_i form mixing definition. Therefore,

$$P_b = J\langle \rho z_* \rangle_V, \qquad M = P_b - P_b(0) - \phi_i t, \tag{5}$$

with $\langle\ \rangle_V$ denoting the volume average. The rate of mixing is $\phi_M = dM/dt$.

The cumulative mixing efficiency, E_c, measures the overall efficiency of mixing over the entire life-cycle of KH billow (Caulfield and Peltier, 2000; Peltier and Caulfield, 2003), and is defined as

$$E_c = \int_T \phi_M dt / (\int_T \phi_M dt + \int_T \varepsilon dt), \tag{6}$$

where T is the duration of interest in the mixing event, and $\varepsilon = \langle (\partial u_i/\partial x_j)^2 \rangle_V / Re_0$ is the dimensionless rate of dissipation of kinetic energy. It is conventional to decompose ε to the rate of dissipation of mean kinetic energy and the rate of dissipation of turbulent kinetic energy: $\varepsilon = \bar{\varepsilon} + \varepsilon^{'}$. To measure the strength of turbulence against stratification, buoyancy Reynolds number is introduced (Smyth and Moum, 2000)

$$Re_b = \frac{\hat{\varepsilon}}{\nu N^2}, \tag{7}$$

where $\hat{\varepsilon} = \varepsilon^{'} \Delta U^3 / \delta_0$ is the dimensional rate of dissipation of turbulent kinetic energy and $N = (-g\Delta\rho/h\rho_0)^{1/2}$ is the buoyancy frequency, with h being the time-varying density layer thickness. Re_b measures both Re_0 and Pr effects.

Variation of mixing, M, and the cumulative mixing efficiency, E_c, with Pr is presented in figure 2 for different Re_0. At $Re_0 = 100$, the total amount of mixing does not depend on Pr due to the dominance of viscous effects. At $Re_0 = 300$, the total amount of mixing increases for higher Pr. This is because finer scale structures at higher Pr make more interfacial area available for mixing and also support more active three-dimensional instabilities. For $Re_0 = 400$ and 600, M decreases with increasing Pr because of the slower rate of molecular diffusion during the active turbulent stages. The cumulative mixing efficiency, E_c, reveals a decreasing trend with increasing Pr, in agreement with the studies of Salehipour et al. (2015), Smyth et al. Smyth et al. (2001) and Stretch et al. (2010). This figure suggests that the mixing efficiency drops at a slower rate at high Pr, where our $Re_0 = 300$ simulations suggest an asymptotic value of 0.05 for high Pr KH billows. Our mixing efficiencies are lower relative to the shown previous DNS studies. We speculate this may be due to the absence of vortex pairing in our simulations. However, our E_c is within the range of measures of mixing efficiency in stratified shear flows from experimental studies (Rottman and Britter, 1986; Rehmann and Koseff, 2004; Fernando, 1991), and field studies (De Lavergne et al., 2015; Bluteau et al., 2013; Lozovatsky and Fernando, 2013) .

Dependence of M and E_c on Re_b (the maximum value each simulation reaches) is examined in figure 3. This figure shows that all our simulations from the present work are in either diffusive or intermediate regime. We have also plotted points from Rahmani et al. (2016) with $Pr = 1$ to provide data points in the energetic regime. This figure delineates a steady increase in M as Re_b increases. In the energetic regime the dependence of M on Re_b becomes less significant. As previously suggested by Shih et al. (2005), Re_b is a good measure for characterizing M. Our trend of variation of E_c with Re_b is similar to the results of Shih et al. (2005). The sharp decrease in E_c in the beginning of the intermediate regime is caused by high Pr flows. E_c increases steadily in the intermediate regime, and reaches a plateau in the energetic regime.

5 Conclusions

We have studied the effects of Pr on mixing in KH billows for low to intermediate Reynolds numbers. The trend of change of the final amount of mixing with increasing Pr shows

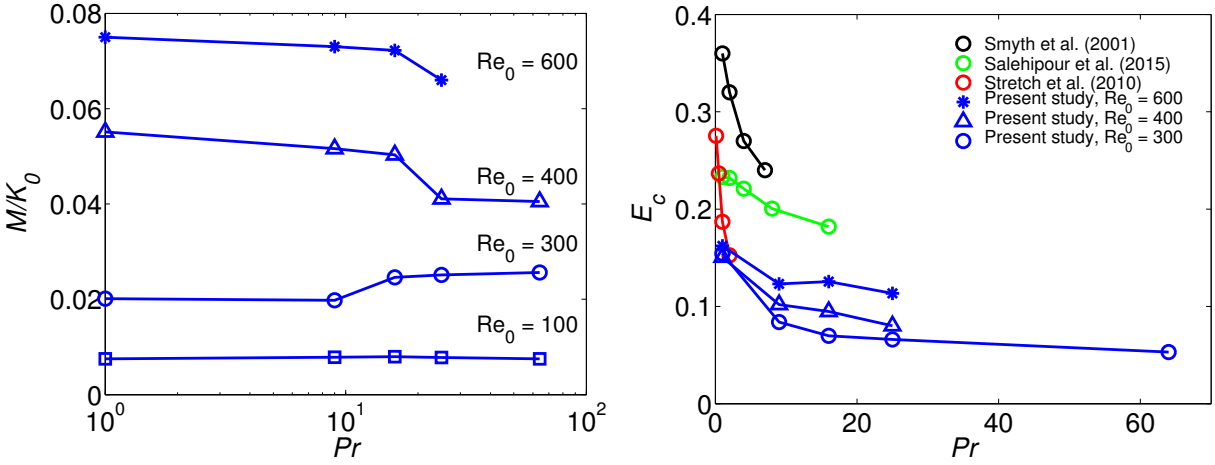

Figure 2: Variation of the total amount of mixing (left) and the cumulative mixing efficiency (right) as a function of the Prandtl number. The left panel shows the variation for different Reynolds numbers: Re_0 = 100, 300, 400 and 600 from bottom to top. The right panel shows E_c as a function of Pr from different KH studies. A part of these results were published in Rahmani et al. (2016).

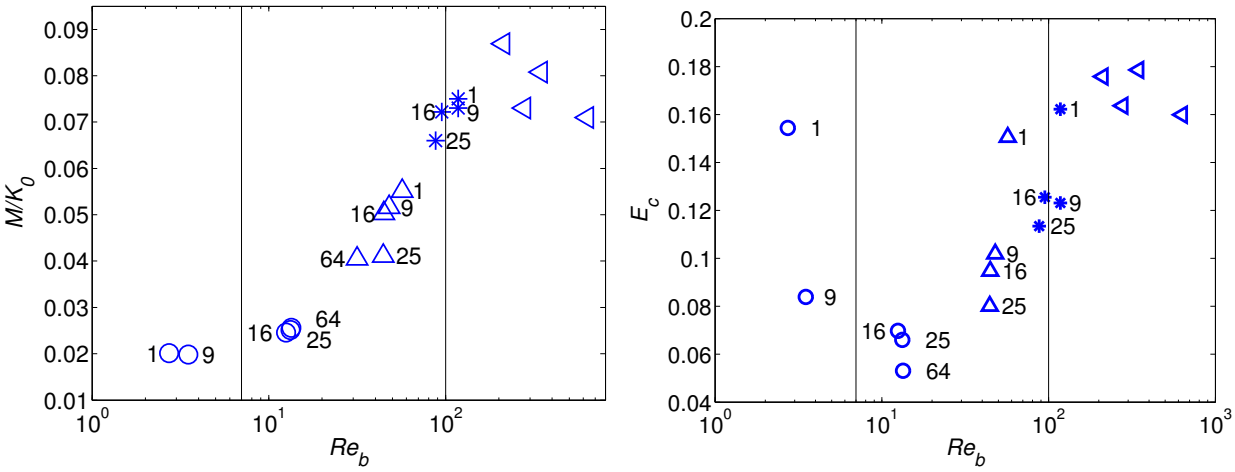

Figure 3: Variation of the total amount of mixing (left) and the cumulative mixing efficiency (right) with maximum buoyancy Reynolds number. The markers indicate different initial Reynolds numbers with different Prandtl numbers: $Re_0 = 300$ (circles), $Re_0 = 400$ (upward-pointing triangles), $Re_0 = 600$ (stars), and higher Re_0 simulations with $Pr = 1$ from Rahmani et al. (2014a) (left-pointing triangles). The number next to each data point shows the Prandtl number. The vertical lines in the left panel show the transition from diffusive to intermediate and from intermediate to energetic mixing regime in the classification of Shih et al. Shih et al. (2005). A part of these results were published in Rahmani et al. (2016).

two distinct behaviours depending on whether the Reynolds numbers at $Pr = 1$ are below or within the mixing transition. For $Re_0 = 300$, the flow is below the mixing transition at $Pr = 1$ and the shearing is not strong enough to overcome viscous effects. For this Reynolds number, the three-dimensional motions and interfacial area are enhanced as Pr rises, resulting in an increase in mixing. For $Re_0 \geqslant 400$, the flow is within the mixing transition at $Pr = 1$ and the the flow actively supports strong three-dimensional for all Prandtl numbers. For such flows, the slower rate of molecular diffusion at higher Pr is more dominant compared to the effect of enhanced interfacial area. Hence, the total amount of mixing decreases as Pr rises.

The buoyancy Reynolds number describes the trends of mixing and mixing efficiency well by representing both Reynolds and Prandtl number effects. Our buoyancy Reynolds numbers for transitions in mixing and mixing efficiency trends match the transitional buoyancy Reynolds numbers of 7 and 100 suggested by Shih et al. (2005). The decreasing trend of the cumulative mixing efficiency with increasing Pr from our DNS matches those of Smyth et al. (2001), Salehipour et al. (2015) and Stretch et al. (2010).

References

Atsavapranee, P. and Gharib, M. (1997). Structures in stratified plane mixing layers and the effects of cross-shear small-scale variation of convected quantities like temperature in turbulent fluid. *Journal of Fluid Mechanics*, 342:53–86.

Balmforth, N., Llewellyn Smith, S. G., and Young, W. (1998). Dynamics of interfaces and layers in a stratified turbulent fluid. *Journal of Fluid Mechanics*, 355:329–358.

Balmforth, N., Roy, A., and Caulfield, C. (2012). Dynamics of vorticity defects in stratified shear flow. *Journal of Fluid Mechanics*, 694:292–331.

Barry, M. E., Ivey, G. N., Winters, K. B., and Imberger, J. (2001). Measurements of diapycnal diffusivities in stratified fluids. *Journal of Fluid Mechanics*, 442:267–291.

Batchelor, G. K. (1959). Small-scale variation of convected quantities like temperature in turbulent fluid. *Journal of Fluid Mechanics*, 5:113–133.

Bluteau, C., Jones, N., and Ivey, G. (2013). Turbulent mixing efficiency at an energetic ocean site. *Journal of Geophysical Research: Oceans*, 118(9):4662–4672.

Breidenthal, R. (1981). Structure in turbulent mixing layers and wakes using a chemical reaction. *Journal of Fluid Mechanics*, 109:1–24.

Caulfield, C. P. and Peltier, W. R. (2000). The anatomy of the mixing transition in homogeneous and stratified free shear layers. *Journal of Fluid Mechanics*, 413:1–47.

Cortesi, A. B., Smith, B. L., Yadigaroglu, G., and Banerjee, S. (1999). Numerical investigation of the entrainment and mixing processes in neutral and stably-stratified mixing layers. *Physics of Fluids*, 11:162–184.

De Lavergne, C., Madec, G., Le Sommer, J., Nurser, A. G., and Naveira Garabato, A. C. (2015). The impact of a variable mixing efficiency on the abyssal overturning. *Journal of Physical Oceanography*, (2015).

Dimotakis, P. E. (2005). Turbulent mixing. *Annual Review of Fluid Mechanics*, 37:329–356.

Fernando, H. J. (1991). Turbulent mixing in stratified fluids. *Annual Review of Fluid Mechanics*, 23(1):455–493.

Klaassen, G. P. and Peltier, W. R. (1985). The onset of turbulence in finite-amplitude Kelvin-Helmholtz billows. *Journal of Fluid Mechanics*, 155:1–35.

Konrad, J. H. (1977). *An experimental investigation of mixing in two-dimensional turbulent shear flows with applications to diffusion-limited chemical reactions*. PhD thesis, California Institute of Technology.

Koochesfahani, M. M. and Dimotakis, P. E. (1986). Mixing and chemical reaction in a turbulent liquid mixing layer. *Journal of Fluid Mechanics*, 170:83–112.

Lozovatsky, I. and Fernando, H. (2013). Mixing efficiency in natural flows. *Philosophical Transactions of the Royal Society of London A: Mathematical, Physical and Engineering Sciences*, 371(1982):20120213.

Lozovatsky, I., Roget, E., Fernando, H., Figueroa, M., and Shapovalov, S. (2006). Sheared turbulence in a weakly stratified upper ocean. *Deep Sea Research Part I: Oceanographic Research Papers*, 53(2):387–407.

Mashayek, A. and Peltier, W. (2011). Three-dimensionalization of the stratified mixing layer at high reynolds number. *Physics of Fluids (1994-present)*, 23(11):111701.

Mashayek, A. and Peltier, W. (2012). The zoo of secondary instabilities precursory to stratified shear flow transition. part 1 shear aligned convection, pairing, and braid instabilities. *Journal of Fluid Mechanics*, 708:5–44.

Nash, J. D. and Moum, J. N. (2002). Microstructure estimates of turbulent salinity flux and the dissipation spectrum of salinity. *Journal of Physical Oceanography*, 32(8):2312–2333.

Park, Y.-G., Whitehead, J., and Gnanadeskian, A. (1994). Turbulent mixing in stratified fluids: layer formation and energetics. *Journal of Fluid Mechanics*, 279:279–311.

Peltier, W. R. and Caulfield, C. P. (2003). Mixing efficiency in stratified shear flows. *Annual Review of Fluid Mechanics .*, 35:135–167.

Rahmani, M., Lawrence, G., and Seymour, B. (2014a). The effect of Reynolds number on mixing in Kelvin–Helmholtz billows. *Journal of Fluid Mechanics*, 759:612–641.

Rahmani, M., Seymour, B., and Lawrence, G. (2014b). The evolution of large and small-scale structures in Kelvin-Helmholtz instabilities. *Environmental Fluid Mechanics*, 14(6):1275–1301.

Rahmani, M., Seymour, B., and Lawrence, G. (2016). The effect of prandtl number on mixing in low reynolds number kelvin-helmholtz billows. *Physics of Fluids*, 28(5):054107.

Rehmann, C. R. and Koseff, J. R. (2004). Mean potential energy change in stratified grid turbulence. *Dynamics of Atmospheres and Oceans*, 37(4):271–294.

Rottman, J. and Britter, R. (1986). The mixing efficiency and decay of grid-generated turbulence in stably-stratified fluids. *Proceedings of the 9th Australasian Fluid Mechanics Conference*.

Salehipour, H., Peltier, W., and Mashayek, A. (2015). Turbulent diapycnal mixing in stratified shear flows: the influence of Prandtl number on mixing efficiency and transition at high Reynolds number. *Journal of Fluid Mechanics*, 773:178–223.

Schowalter, D. G., Atta, C. W. V., and Lasheras, J. C. (1994). A study of streamewise vortex structure in a stratified shear layer. *Journal of Fluid Mechanics*, 281:247–291.

Shih, L. H., Koseff, J. R., Ivey, G. N., and Ferziger, J. H. (2005). Parameterization of turbulent fluxes and scales using homogeneous sheared stably stratified turbulence simulations. *Journal of Fluid Mechanics*, 525:193–214.

Smyth, W., Moum, J., and Caldwell, D. (2001). The efficiency of mixing in turbulent patches: inferences from direct simulations and microstructure observations. *Journal Physical Oceanography*, 31:1969–1992.

Smyth, W. D. and Moum, J. N. (2000). Length scales of turbulence in stably stratified mixing layers. *Physics of Fluids*, 12:1327–1342.

Spigel, R. H. and Imberger, J. (1980). The classification of mixed-layer dynamics of lakes of small to medium size. *Journal of physical oceanography*, 10(7):1104–1121.

Staquet, C. (2000). Mixing in a stably stratified shear layer: two- and three-dimensional numerical experiments. *Fluid Dynamics Research*, 27:367–404.

Stretch, D. D., Rottman, J. W., Venayagamoorthy, S. K., Nomura, K. K., and Rehmann, C. R. (2010). Mixing efficiency in decaying stably stratified turbulence. *Dynamics of Atmospheres and Oceans*, 49(1):25–36.

Winters, K. B., Lombard, P. N., Riley, J. J., and D'asaro, E. A. (1995). Available potential energy and mixing in density-stratified fluids. *Journal of Fluid Mechanics*, 289:115–128.